BACKFILLING OF SANDY COAST BREACHING AFTER THE 2011 TSUNAMI

Vo Cong Hoang[1], Hitoshi Tanaka[2], Yuta Mitobe[3], Keiko Udo[4] and Akira Mano[5]

Breaching of sandy coast was commonly observed on Yamamoto Coast, southern Miyagi Prefecture during the 2011 tsunami. That made the shoreline having concave shape after the tsunami. Concave shoreline is bounded by two headlands. The recovery of concave shoreline is discussed through the analysis of satellite images. The relationship between dimensionless elapsed time with dimensionless recovery of shoreline at the central line of concave portion, and dimensionless of area of backfilling in the concave portion are studied based on analytical solutions of the one-line model. For those two relationships, results obtained for case with rigid boundaries is asymptotic when the ratio between length of the bounded coast and width of concave portion is getting larger. Good agreement between measured data and theoretical results can be obtained.

Keywords: Tsunami, Yamamoto Coast, concave shoreline, analytical solution, one-line model

INTRODUCTION

The tsunami, which occurred on March 11, 2011, caused severe damages of coastal morphology in the northeast area of Japan. The significant changes and subsequent recovery of estuarine and coastal morphology in Miyagi Prefecture were reported by numerous researchers (e.g. Tanaka et al., 2012; Udo et al., 2012 and 2015; Tappin et al., 2012). One of the most typical damages commonly observed on Yamamoto Coast, which is located in the south of Miyagi Prefecture, was the breaching of sandy coast (Udo et al., 2015). Due to this tsunami-induced damage, shoreline after the tsunami had concave shape. Subsequently, fast recovery of some breaching could be observed. However at many other places, the recovery of breaching was not observed. Along Yamamoto Coast, significant erosion occurred from 1970s in response to the erosion protection of cliff coast in Fukushima Prefecture which was considered as main sediment source to maintain the shoreline of Yamamoto Coast. In order to prevent the erosion on this coast, starting from 1990s until before the tsunami, 7 groins and 2 headlands have been constructed (Udo et al., 2015). Therefore, the effects of these coastal structures to the recovery process of morphology need to be considered in this case.

Analytical solutions of one-line model have been developed and utilized widely in the computation of coastal morphology evolution. For the evolution of concave shoreline, Larson et al. (1987) introduced analytical solution of one-line model for case without rigid boundaries at both ends of concave region, whereas Hoang et al. (2015a) proposed analytical solution for case with rigid boundaries. Discussion on the relationship and applicability of them is still lack so far. Furthermore, these solutions are also very useful for engineering application, especially, in the case of beach nourishment (e.g. Dean, 2003).

Taking all together, this study investigates the recovery of concave morphology bounded by headlands on Yamamoto Coast through analysis of satellite images and analytical solutions of one-line model.

STUDY AREA & DATA COLLECTION

This study mainly focuses on the beach of about 1000 m in length on Yamamoto Coast which is located on the south of Miyagi Prefecture, Japan (Figure 1). It is located about 7 km in the south of the Abukuma River mouth and bounded by two headlands No. 9 (south) and No. 11 (north).

Satellite images, which are utilized in this study, are downloaded from Google Earth. Collected satellite images are re-rectified to the World Geodetic System (WGS-84). A shore-parallel line, which is 178^o clockwise from the north, was taken as the baseline for shoreline position measurement. Shoreline position, which is represented by wet/dry line, is extracted based on the difference of color intensity between water and land sides. All extracted shoreline positions were not corrected to tidal level due to the lack exact time of capture.

[1] Department of Hydraulic Structure, Thuyloi University-Southern Campus, 02 Truong Sa, Ward 17, Binh Thanh District, Ho Chi Minh City, Vietnam
[2] Department of Civil Engineering, Tohoku University, 6-6-06 Aoba, Sendai 980-8579, Japan
[3] Department of Civil Engineering, Tohoku University, 6-6-06 Aoba, Sendai 980-8579, Japan
[4] International Research Institute of Disaster Science, Tohoku University, 6-6-11 Aoba, Sendai, Japan
[5] Emeritus Professor, International Research Institute of Disaster Science, Tohoku University, 6-6-11 Aoba, Sendai, Japan

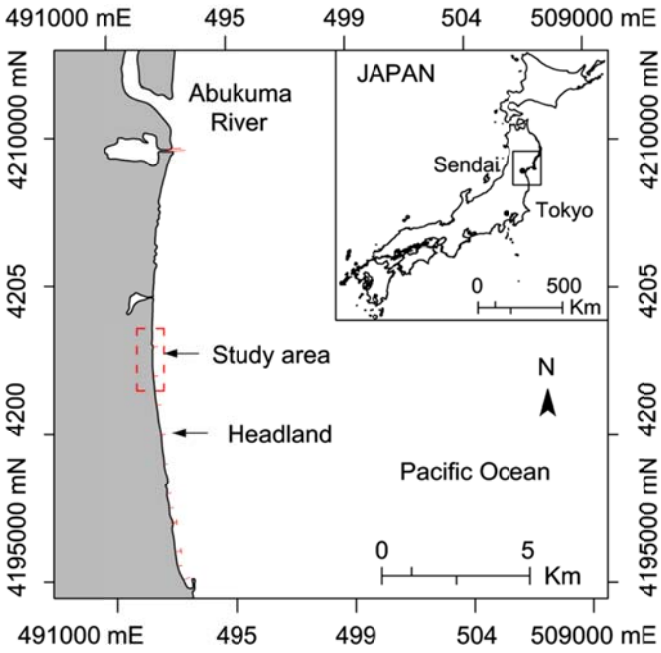

Figure 1. Location map of study area

MORPHOLOGICAL RECOVERY AFTER THE TSUNAMI

Overviews of coastal morphology damages and subsequent recovery on entire Yamamoto Coast were presented in Udo et al. (2015). This study investigates more details on the recovery of the area of about 1000 m between headlands No. 9 and 11.

Figure 2 shows selected satellite images of breaching on Yamamoto Coast. Before the tsunami, the landward part was covered by pine tree forest (Figure 2(a)). Figure 2(b) shows the morphology 3 days after the tsunami. The pine tree forest has been swashed. A longshore canal can be seen clearly from this image. This canal was created from the erosion behind the seawall (Udo et al., 2015). Beaching of sandy coast also can be observed. Its width was about 110 m. Due to the existence of this breaching, shoreline in this area has concave form. The recovery of morphology in this area was rather fast (Figures 2(c), (d) and (e)). During the recovery process, the alongshore canal was blocked by the sediment transported into the breaching. Figure 2(f) indicates that the recovery of breaching has been completed. The elevating of seawall (+7.2 m, Tokyo Peil) in this area has been completed as shown in Figure 2(g). Shoreline positions before the tsunami and during the recovery process, which were extracted from aerial photographs shown in Figure 2, are shown in Figure 3. During the recovery process, shoreline position in the concave portion was advance while shoreline positions of adjacent sandy coasts were retreat. This behavior is similar to the one of concave shoreline recovery presented in Hoang et al. (2015a). Figure 4 shows an oblique photograph of the breaching which was taken about 20 days after the tsunami. It confirms the connecting of the breaching and the blocking of canal by the sediment transported into the concave portion. Another oblique photograph is shown in Figure 5. It indicates that the beaches which are adjacent to the breaching were eroded (dashed circle line). It has the form of cliff beach. From this and the behavior of shoreline evolution presented in Figure 3, it can be said that during the recovery process of the breaching, sediment on adjacent beaches was transported into the concave portion; hence the longshore sediment transport is dominant in this case.

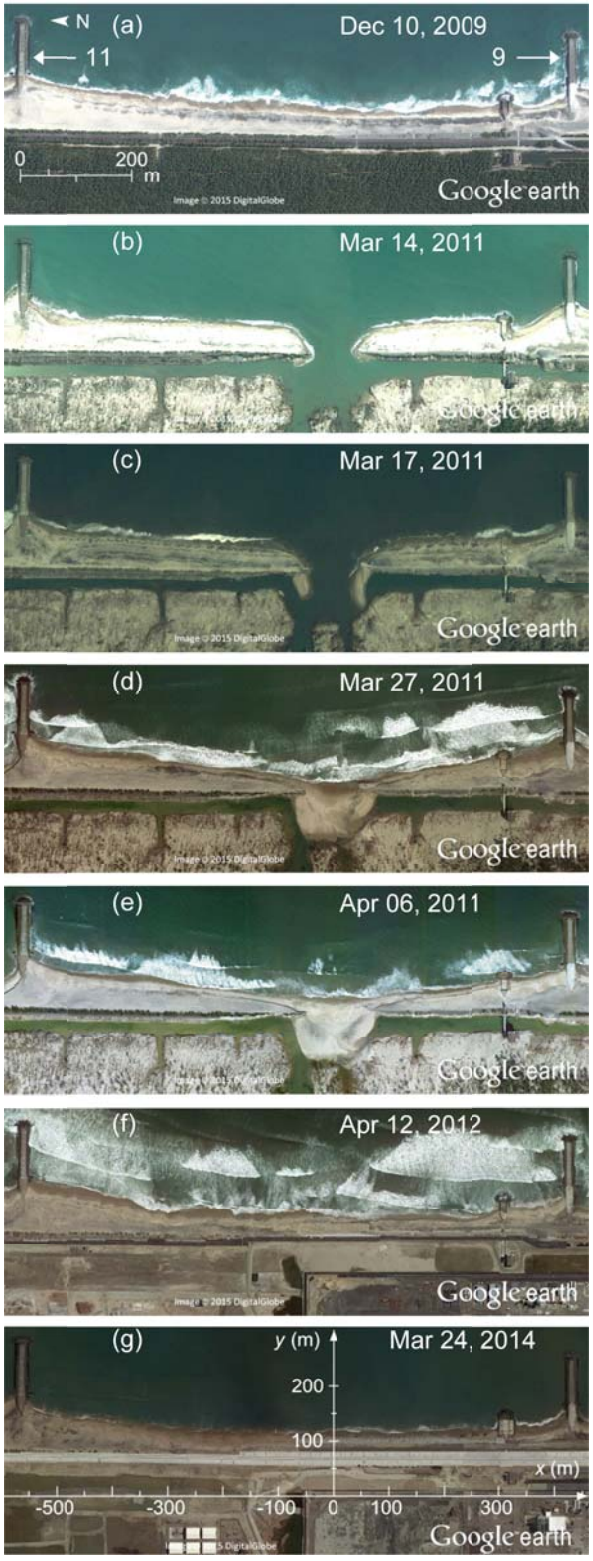

Figure 2. Selected satellite images of breaching on Yamamoto Coast and its subsequent recovery process (Google Earth)

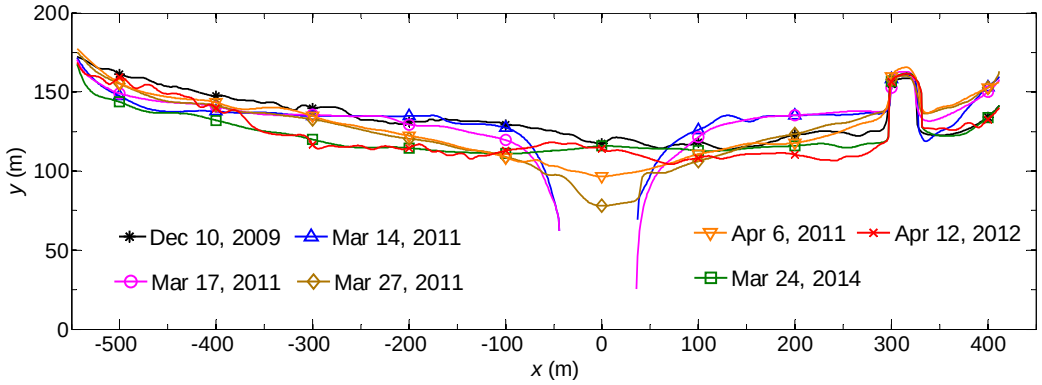

Figure 3. Detected shoreline positions of the study area

Figure 4. Oblique photograph showing the recovery of concave shoreline on Yamamoto Coast after the tsunami (Taken: April 2, 2011)

Figure 5. Erosion of beach adjacent to the breaching after the tsunami (cliff beach) (Taken: April 2, 2011)

BACKFILLING OF SEDIMENT INTO THE CONCAVE PORTION

Analytical solutions on backfilling of sediment

As mentioned previously, during the recovery process of concave shoreline, longshore sediment is predominant. In addition, in entire concave shoreline region the intensity of shoreline variability is high because of imbalance of shoreline at the concave portion induced by the tsunami; hence the evolution of concave shoreline can be described by the theory of one-line model. The one-line model, which was derived based on the principle of mass conservation, considers the beach having parallel depth contours from the berm to the depth of closure. Based on that governing equation of one-line model is given as Eq. (1).

$$\frac{\partial y}{\partial t} = -\frac{1}{D_B + D_C}\frac{\partial Q}{\partial x} \tag{1}$$

where Q is longshore sediment transport rate; D_B is height of berm; D_C is depth of closure; x and y (Figure 6) are the coordinates along baseline and the shoreline positions (distance from baseline to shoreline on transections), respectively; t is time.

Simplified governing equation of the one-line model, Eq. (2), can be obtained based on the assumptions that angle of wave breaking crests to local shoreline is supposed to be small, and breaking

wave characteristics are assumed to be constant along the coast (independent of x and t). More details on how to derive the simplified governing equation of one-line model from Eq. (1) can be found in Larson et al. (1987).

$$\frac{\partial y}{\partial t}=\varepsilon\frac{\partial^2 y}{\partial x^2} \tag{2}$$

where ε is diffusion coefficient, and it is given by the following equation.

$$\varepsilon=\frac{K(H^2C_g)_b}{8}\frac{\rho}{\rho_s-\rho}\frac{1}{1-n}\frac{1}{D_C+D_B} \tag{3}$$

where K is dimensionless empirical proportionality coefficient in longshore sediment transport rate formula; H is wave height, C_g is wave group celerity, the subscript "b" denotes for the quantity at the breaking line; ρ_s is mass density of the sediment grains; ρ is mass density of water; n is sediment porosity.

Larson et al. (1987) and Hoang et al. (2015a) presented the analytical solutions of one-line model which describe the evolution of concave shoreline for cases without and with rigid boundaries at both ends as Eqs. (4) and (5), respectively.

$$y=\frac{1}{2}Y_0\left[erfc\left(\frac{B-2x}{4\sqrt{\varepsilon t}}\right)+erfc\left(\frac{B+2x}{4\sqrt{\varepsilon t}}\right)\right] \tag{4}$$

$$y=Y_0\left[1-\frac{B}{L}-\frac{2}{\pi}\sum_{n=1}^{\infty}\frac{1}{n}\sin\frac{n\pi B}{L}exp\left(-\frac{4\varepsilon n^2\pi^2 t}{L^2}\right)\cos\frac{2n\pi x}{L}\right] \tag{5}$$

where Y_0 is the cross-shore distance of the beach cut region from the initial shoreline. It is estimated based on the actual condition of shoreline right after the tsunami; *erfc* is the complementary error function; B is width of concave portion; L is total length of sandy coast bounded by two headlands. It is noted that the headlands are treated as rigid boundaries which completely block the movement of longshore sediment (no longshore sediment transported in/out the area bounded by headlands); the condition $\partial y/\partial x=0$ is applied at the headlands. The evolution of shoreline positions plotted from Eqs. (4) and (5) can be found in Hoang et al. (2015a).

As mentioned earlier, during the recovery process, the concave portion was step by step backfilled by the sediment from adjacent sandy beaches. This backfilling can be expressed in term of the proportional recovery of shoreline position at the central line of concave portion (y_c/Y_0) or the proportional area of concave portion filled by sediment from adjacent coasts, P_A.

The backfilling of sediment into the concave portion was previously presented in Hoang et al. (2015b). In that study, concave shorelines at Akaiko Coast and at the Nanakita River mouth, which are located in the north of current study area, were taken as study areas.

In case considering the proportional recovery of shoreline at the central line of concave portion, analytical solution for cases without and with rigid boundaries at both ends can be obtained from Eqs. (4) and (5) as Eqs.(6) and (7), respectively.

$$y^*=erfc\left(\frac{1}{4t^*}\right) \tag{6}$$

$$y^*=\left[1-\frac{1}{L^*}-\frac{2}{\pi}\sum_{n=1}^{\infty}\frac{1}{n}sin\frac{n\pi}{L^*}exp\left(-\frac{4n^2\pi^2t^{*2}}{L^{*2}}\right)\right] \tag{7}$$

where dimensionless parameters are defined below

$$y^*=y_C/Y_0 \tag{8}$$

$$t^*=\sqrt{\varepsilon t}/B \tag{9}$$

$$L^*=L/B \tag{10}$$

In case of considering the proportional area backfilling, Dean (2003) and Hoang et al. (2015b) proposed analytical solutions of the one-line model to estimate P_A for cases without and with rigid boundaries at both ends as Eqs. (11) and (12), respectively.

$$P_A = 1 - \frac{2t^*}{\sqrt{\pi}}\left\{exp\left[-\left(\frac{1}{2t^*}\right)^2\right] - 1\right\} - erf\left(\frac{1}{2t^*}\right) \tag{11}$$

$$P_A = \frac{2L^{*2}}{(L^* - 1)\pi^2}\sum_{n=1}^{\infty}\frac{1}{n^2}sin^2\frac{n\pi}{L^*}\left[1 - exp\left(-\frac{4n^2\pi^2 t^{*2}}{L^{*2}}\right)\right] \tag{12}$$

In case with rigid boundaries, the sediment is considered as the sediment filled into the concave portion before shoreline position in the concave portion gets equilibrium stage.

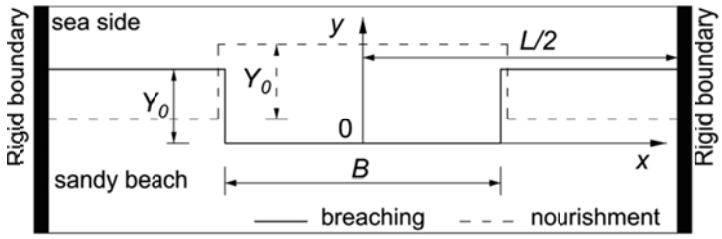

Figure 6. Schematic diagram of concave shoreline on beach bounded by headlands (rigid boundaries)

Comparing the analytical solutions on the recovery of concave shoreline

Figure 7(a) shows the relationship between t^* and y^* for case recovery of concave shoreline. When considering a particular ratio of L/B, the relationship between t^* and y^* obtained from cases of without and with rigid boundaries (Eqs. (6) and (7)) are overlapping each other while t^* is small. This indicates that the evolution of shoreline has not been influenced by the rigid boundaries yet. However, when t^* is getting larger they are much different; the influence of rigid boundaries are shown clearly. In case of large t^*, if L/B is getting larger, the relationship between t^* and y^* obtained from the case with rigid boundaries (Eq. 7) is asymptotic with the relationship obtained from case without rigid boundaries (Eq. 6). Figure 7(b) shows the relationship between t^* and P_A for case of recovery of concave shoreline. When L/B is getting larger, the relationship obtained from the case with rigid boundaries is asymptotic with the one of case without rigid boundaries. It is noted that in Figures 7(a) and (b) the relationships obtained from case with rigid boundaries get stable very early (no further significant recovery). Those points, which indicate the no significant further recovery points, are presently exampled by the vertical arrows in Figure 7(a). This is distinct difference with the ones obtained from the case without rigid boundaries. On the other hand, measured data, which was extracted from satellite images of the concave shoreline of the study area (L/B=8.8), is also presented in Figures 7(c) and (d). Good agreement between theoretical results obtained from case with rigid boundaries and measured data, especially when t^* is large. The disagreement when t^* is small can be attributed by several reasons; they would be the complicated geometry of concave portion after the tsunami and the difference of wave characteristics with its constant conditions assumed when applying theory of one-line model.

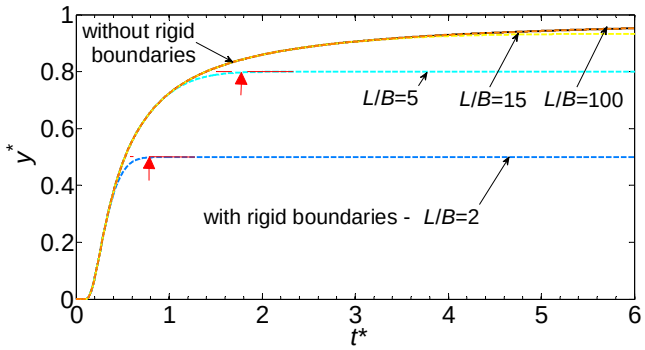

(a) Relationship between *t and y^***

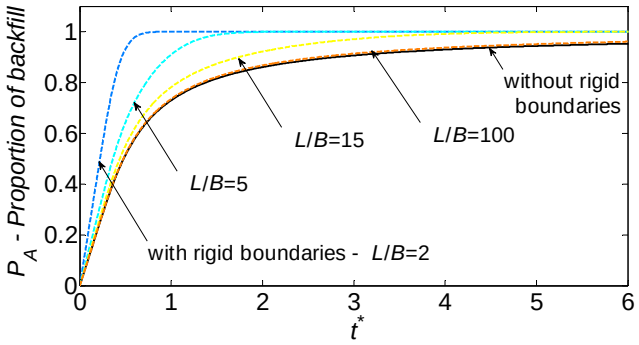

(b) Relationship between *t and P_A**

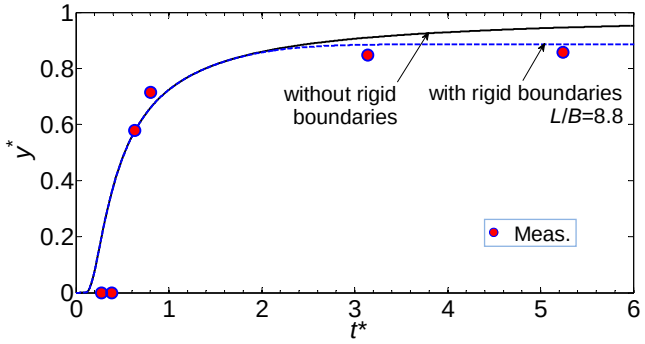

(c) Relationship between *t and y^* with measured data**

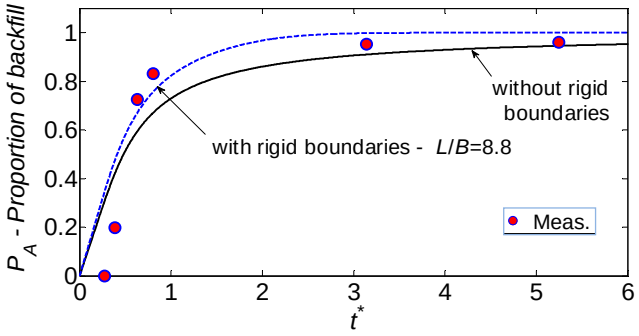

(d) Relationship between *t and *PA***

Figure 7. Relationships between *t and y^*, and between *t** and P_A for case of concave shoreline**

Application to case of beach nourishment

Theory on the backfilling of sediment into the concave portion is not only important for the recovery of concave shoreline case but also very useful in case of beach nourishment. It is interesting to

know that by making slightly modification, the mentioned theory can describe the remaining of sediment in the nourished area in the process of rectangular planform beach nourishment. Equations, which describe the proportional decreasing of shoreline position at the central line of nourished area (convex portion), y_N^*, for cases without and with rigid boundaries at both ends, can be obtained from Eq. (13) when using corresponded y^* from Eqs. (6) and (7).

$$y_N^* = 1 - y^* \tag{13}$$

By applying similar approach, the proportion area of sediment remaining in the convex portion before shoreline position in this area reach the equilibrium stage, P_{AN}, for cases without and with rigid boundaries, can be obtained from Eq. (14) when utilizing appropriate P_A from Eqs. (11) and (12).

$$P_{AN} = 1 - P_A \tag{14}$$

Figures 8(a) and (b) show the relationship between t^* and y_N^* (Eq. (13)) and t^* and P_{AN} (Eq. (14)) for cases without and with rigid boundaries in case of beach nourishment. In that case, the remaining of sediment in the nourished area (convex portion) is considered. It is similar to case of concave shoreline recovery that the relationships between t^* and y_N^*, and t^* and P_{AN} obtained from case with rigid boundaries are asymptotic with those for case without rigid boundaries. The behavior of fast getting stable (no further significant decreasing) also can be found in this case.

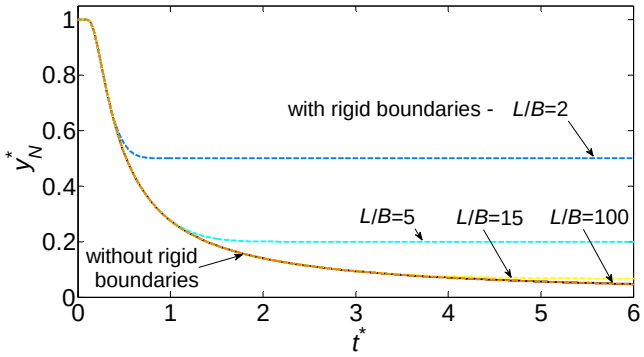

(a) Relationship between t^* and y_N^*

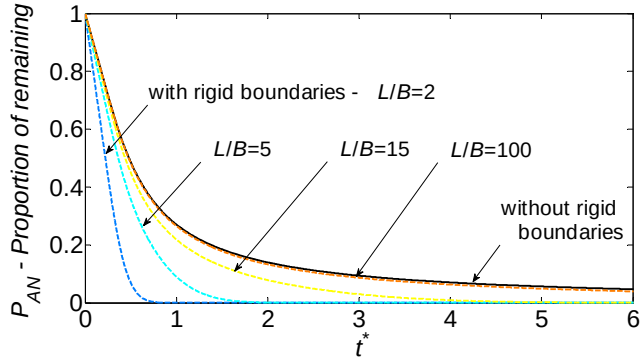

(b) Relationship between t^* and P_{AN}

Figure 8 Relationships between t^* and y_N^*, and between t^* and P_{AN} for case of rectangular planform beach nourishment

CONCLUSIONS

In this study, the recovery of a concave shoreline on Yamamoto Coast, southern Miyagi Prefecture after the tsunami has been studied. The concave shoreline has recovered rather fast. Within a few months, the concave portion has been almost fully backfilled. The relationships between t^* and y^*, and

t^* and P_A for case with rigid boundaries get stable very early (no further significant recovery) compared to the case of without rigid boundaries. This is distinct difference between them. When the dimensionless recovery time is large and ratio between the length of beach bounded by two headlands and the width of concave portion is also large, the relationships between t^* and y^*, and t^* and P_A for cases without and with rigid boundaries are asymptotic together. Comparison between measured data and theoretical results has been done. Good agreement can be obtained when the dimensionless elapsed time is large. Applicability of above theory in the process of beach nourishment has been also introduced.

ACKNOWLEDGEMENTS

This work was supported by Foundation of River and Watershed Environmental Management (FOREM). Authors would like to express their gratitude to the above support.

REFERENCES

Dean, R. 2003. *Beach nourishment - theory and practice*, World Scientific, 420p.

Hoang, V.C., H. Tanaka, and Y. Mitobe. 2015a. Theoretical study on the recovery process of the concave landform after the tsunami, *Journal of JSCE, Ser. B1 (Hydraulic Engineering),* 71(4), I_31-I_36.

Hoang, V.C., H. Tanaka, and Y. Mitobe. 2015b. Theory for backfilling of tsunami-induced beach erosion. *Journal of JSCE, Ser. B3 (Ocean Engineering)*, 71, CD-ROM.

Larson, M., H. Hanson, and N.C. Kraus. 1987. Analytical solutions of the one-line model of shoreline change, *Technical Report CERC-87-15*, U.S. Army Engineer Waterways Experiment Station.

Tanaka, H., N.X. Tinh, M. Umeda, R. Hirao, E. Pradjoko, A. Mano, and K. Udo. 2012. Coastal and estuarine morphology changes induced by the 2011 Great East Japan earthquake tsunami, *Coastal Engineering Journal,* 54(1), 1250010 (25 pages).

Tappin, D.R., H.M. Evans, C.J. Jordan, B. Richmond, D. Sugawara, and K. Goto. 2012. Coastal changes in the Sendai area from the impact of the 2011 Tōhoku-oki tsunami: Interpretations of time series satellite images, helicopter-borne video footage and field observations, *Sedimentary Geology,* 282(30), 151-174.

Udo, K., D. Sugawara, H. Tanaka, K. Imai, and A. Mano. 2012. Impact of the 2011 Tohoku Earthquake and Tsunami on beach morphology along the northern Sendai Coast *Coastal Engineering Journal,* 54(01), 1250009 (15 pages).

Udo, K., Y. Takeda, M. Takamura, and A. Mano. 2015. Serious erosion of the southern Sendai Coast due to the 2011 Tohoku Earthquake Tsunami and its recovery process. *in Santiago-Fandino, V., Konta, Y. A., Kaneda, Y., (Eds.), Springer, Post-Tsunami Hazard - Reconstruction and Restoration,* 44, 225-236.